Prokaryotic origin of the actin cytoskeleton

Fusinita van den Ent, Linda A. Amos & Jan Löwe

MRC Laboratory of Molecular Biology, Hills Road, Cambridge CB2 2QH, UK

It was thought until recently that bacteria lack the actin or tubulin filament networks that organize eukaryotic cytoplasm. However, we show here that the bacterial MreB protein assembles into filaments with a subunit repeat similar to that of F-actin—the physiological polymer of eukaryotic actin. By elucidating the MreB crystal structure we demonstrate that MreB and actin are very similar in three dimensions. Moreover, the crystals contain protofilaments, allowing visualization of actin-like strands at atomic resolution. The structure of the MreB protofilament is in remarkably good agreement with the model for F-actin, showing that the proteins assemble in identical orientations. The actin-like properties of MreB explain the finding that MreB forms large fibrous spirals under the cell membrane of rod-shaped cells, where they are involved in cell-shape determination. Thus, prokaryotes are now known to possess homologues both of tubulin, namely FtsZ, and of actin.

A central component of the eukaryotic cytoskeleton is filamentous actin. Actin is the most abundant protein in many eukaryotic cells, and is conserved from yeast to humans[1]. In 1942, Straub isolated monomeric actin (G-actin) and discovered that raising the salt concentration causes G-actin to polymerize into filamentous actin (F-actin)[2]. Electron microscopy and X-ray fibre diffraction have shown that F-actin consists of two protofilaments that are twisted gently around one another to form a right-handed double helix. The subunits in each actin protofilament have an approximately 55 Å spacing[3], and the helical pitch is variable owing to torsional flexibility of the protofilaments[4]. Under appropriate conditions actin will polymerize into a variety of polymers[5]. When actin is treated with gadolinium it assembles into sheets and cylinders of straight protofilaments[6]. The filamentous polymers of actin determine the shape of many eukaryotic cells, besides having a vast range of other functions. The three-dimensional structure of G-actin—which has a relative molecular mass of 43,000 (M_r 43K)—has been determined in complexes with various actin-binding proteins that prevent actin polymerization[7–10].

Actin is a member of a larger superfamily of proteins[11,12], which includes Hsp70 (ref. 13), cell-division protein FtsA[14], and sugar kinases[15,16]. Crystal structures have revealed that each member of the actin superfamily has the characteristic core of actin, and is distinguished by additional insertions or deletions that are necessary for the specific function of each family member. A sequence database search revealed that the bacterial proteins MreB and StbA have sequence patterns in common with the actin superfamily[11]. MreB, among all proteins of the superfamily, is most closely related to actin in overall size[11].

The *mreB* gene is located in the gene cluster *mre* (murein cluster e). It is, together with *mrd*, the principal operon involved in determination of cell shape in bacteria[17–19]. Recent evidence shows that MreB assembles into a cytoskeleton-like structure in *Bacillus subtilis*[20]. MreB and the closely related protein Mbl are important in regulating the cell shape of *B. subtilis*; immunofluorescence reveals that elongated polymers of MreB and Mbl encircle the cell as large spirals under the cell membrane. The MreB proteins are widely distributed among rod-shaped, filamentous and helical bacteria[20], suggesting that an MreB cytoskeleton is important to generate a non-spherical shape.

To investigate whether MreB can self assemble into actin-like filaments, we cloned and purified MreB from *Thermotoga maritima*. Biochemical and electron microscopic analyses show that the protein forms filaments with a longitudinal repeat similar to that of eukaryotic actin. Elucidation of the crystal structure of MreB shows that it is indeed clearly related to actin. Furthermore, the crystal packing reveals the filamentous structure of an actin-like protein at atomic resolution. Here we provide biochemical and structural evidence for MreB as the bacterial actin homologue.

Polymerization assays

The gene encoding MreB1 from *T. maritima* was amplified by polymerase chain reaction (PCR) and cloned for overexpression in *Escherichia coli* strain C41 (see Methods). *Thermotoga maritima* has two *mreB* genes. We also cloned *mreB2*, but the protein was mostly insoluble (data not shown). A BLAST search with both proteins revealed that MreB1 is more closely related to MreB from *B. subtilis*, with 56% overall identity.

MreB forms polymers under various conditions, as was initially investigated in a pelleting assay (Fig. 1). To polymerize, MreB requires ATP (Fig. 1a, lane 1) or GTP (lane 5). It can form filaments in the absence of magnesium (lane 4). Polymers are formed over a wide pH range, the optimum being pH 6–7 (Fig. 1b). In contrast to actin polymerization, which requires physiological salt concentrations, *T. maritima* MreB is able to form filaments over a wide range of salt concentrations, as high as 4 M NaCl. The fact that thermophilic organisms usually possess relatively high intracellular salt concentrations could explain the ability of *T. maritima* MreB to assemble in high salt.

Electron microscopy

The nature of MreB polymers, found in the pelleting assay, was investigated by electron microscopy of negatively stained samples. A variety of polymers formed under different conditions (see Fig. 2a, e). The simplest polymers are thin filaments that appear to consist of two protofilaments (each composed of a string of monomers), but such individual thin filaments are rare. More common are pairs of thin filaments, which are often curved (Fig. 2a) depending on the conditions used. Those shown in Fig. 2a are much more highly curved than would be required to produce the curved filaments observed *in vivo*[20]. From our images it is unclear how the curvature is accommodated into the structure.

The filtered image (Fig. 2d) of the polymer in Fig. 2b (diameter of about 160 Å) apparently shows two thin filaments, with an approximately 51 Å longitudinal spacing (Fig. 2c). The thin filaments appear to lack the distinct twist of the two-stranded helices of F-actin, although they often appear to have a slight twist. At low NaCl concentrations (25 mM NaCl), MreB forms two-dimensional

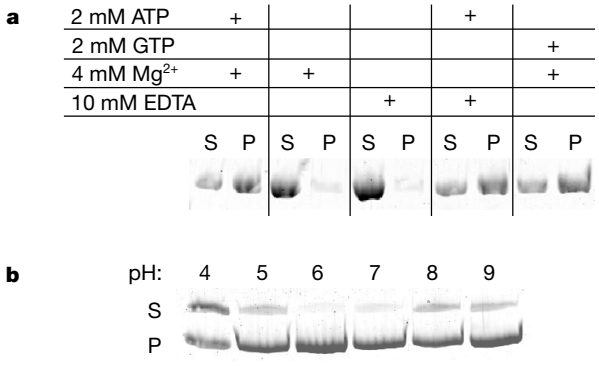

Figure 1 MreB polymerization assays. MreB was incubated at 37 °C with nucleotide and NaCl, and was centrifuged at 140,000*g*. S, supernatant; P, solubilized pellet. Proteins were separated on a 12% SDS gel and stained with PAGE 83. **a**, Effect of nucleotides and magnesium. MreB requires ATP or GTP, but not magnesium, for polymerization. **b**, pH optimum. MreB was incubated under standard conditions (see Methods) with 100 mM buffer: citrate pH 4, pH 5, MES pH 6, HEPES pH 7, Tris-HCl pH 8, BICINE pH 9. Maximal pelleting was observed at pH 6–7.

crystalline sheets (Fig. 2e). The diffraction pattern from the sheets also shows a strong layer line at 51 Å, and in addition a spacing of 39 Å in the equatorial plane (Fig. 2f). Filtered images of the sheets (Fig. 2g) show individual filaments that are consistent with the protofilaments in the crystal structure (see below). They seem to be related to the gadolinium-induced sheets of actin, which consist of untwisted protofilaments arranged in an antiparallel

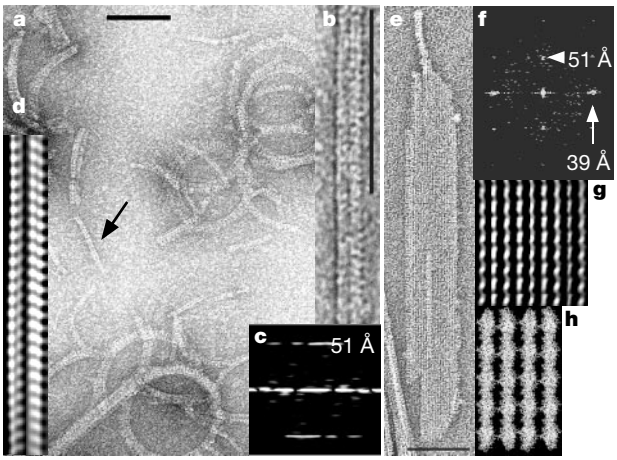

Figure 2 Electron micrographs of negatively stained MreB filaments. **a**, Typical view of MreB filaments when salt and neutral pH is used. MreB (1 mg ml^{-1}) was incubated for 30 min at 37 °C in 100 mM Tris-HCl, pH 7.5, 100 mM NaCl, 3 mM $CaCl_2$, 2 mM ATP (buffered) and 4 mM $MgCl_2$. Scale bar, 100 nm. The filament indicated with an arrow is the same filament that is shown at a higher magnification in **b**. **b**, 'Double' filament formed at high pH. MreB (1 mg ml^{-1}) was incubated for 30 min at 37 °C in 100 mM BICINE, pH 9.0, 100 mM NaCl, 2 mM ATP (buffered) and 4 mM $MgCl_2$. Scale bar, 100 nm. **c**, Diffraction image of the polymer in **b** showing the first strong layer line at 51 Å. **d**, Filtered image of **b**, treating both filaments separately. The polymer is about 160 Å wide, which suggests four single protofilaments in total (each 40 Å, see Fig. 5). **e**, Electron micrograph of a negatively stained MreB sheet. MreB (1 mg ml^{-1}) was incubated for 30 min at 37 °C in 100 mM Tris-HCl, pH 7.5, 25 mM NaCl, 2 mM ATP (buffered) and 4 mM $MgCl_2$. The protofilaments are aligned vertically in the MreB sheet. Scale bar, 100 nm. **f**, Diffraction image of sheet in **e**. The longitudinal repeat is 51 Å, the lateral spacing is 39 Å. **g**, Filtered image of sheet in **e**. **h**, The protofilaments found in the crystals of MreB fit well with the filtered image in **g**. The longitudinal repeat of 51 Å in the sheets is the same as in the crystals (Fig. 5). The lateral spacing in the sheets suggests that the protofilaments interact with their flat sides.

conformation[6]. It is possible, but not yet certain, that the MreB sheets also have an antiparallel arrangement of protofilaments.

The electron microscopic analysis shows that the polymers found in the pelleting assay and in all other tested conditions have a longitudinal spacing of 51 Å, which is reminiscent of the 55 Å spacing of F-actin's helical strands[3].

Crystal structure of MreB

To investigate the homology of MreB to actin in atomic detail, we determined the three-dimensional structure of MreB. We obtained trigonal and monoclinic crystals of MreB from *T. maritima*. The trigonal crystals, space group $P3_121$, diffracted to 2.1 Å but were partially twinned. The structure was solved by multiple anomalous dispersion (MAD), using the monoclinic crystals (space group *C*2, see Methods and Supplementary Information Table 1). The structures of both the apo- (NATI) and AMPPNP-containing trigonal crystals were solved by molecular replacement (Table 1).

The structure of MreB confirms that it is a member of the actin family of proteins, and is characterized by two domains (I and II) that hold a nucleotide-binding site in the interdomain cleft[12]. Each domain is subdivided into two subdomains (A and B) (Fig. 3). The two larger subdomains (IA and IIA) have a common fold that comprises a five-stranded β-sheet surrounded by three α-helices. These subdomains are connected through a helix, H4. The smaller subdomains (IB and IIB) are more diverse in the actin superfamily, and are probably unique to the specific function of the proteins. Notably, MreB shows exactly the same topology as actin in the structure of these domains (Fig. 4). This is in contrast to Hsp70, FtsA and, in particular, the sugar kinases. The position where the smaller subdomains are inserted is identical in the two proteins, that is, after the third strand (S3 and S11, respectively) of the β-meander of both subdomain IA and IIA. One significant difference between actin and MreB is a loop that is inserted in actin in the equivalent of helix H8. The loop has been implicated in the intermolecular interaction between the subunits during initial assembly of the filament[3].

A three-dimensional structural similarity search revealed that MreB can be superimposed on actin (Protein Data Bank (PDB)

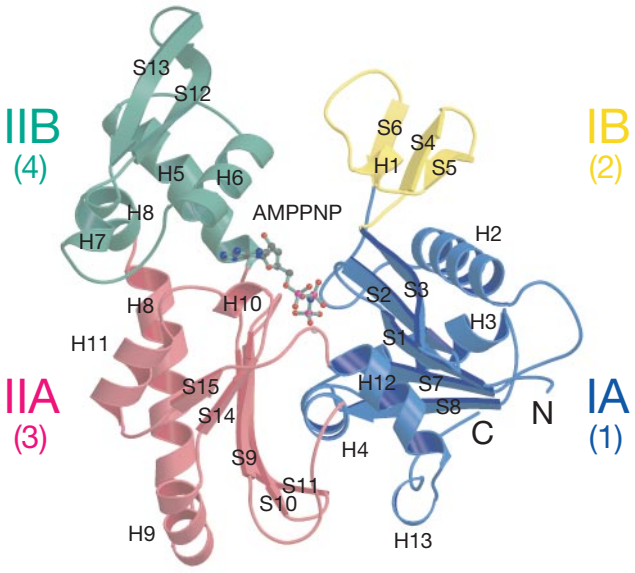

Figure 3 Ribbon representation of the crystal structure of MreB complexed with AMPPNP and magnesium. MreB is a member of the actin family of proteins, showing the typical four-domain architecture. AMPPNP binds in a cleft between domains I and II. The four subdomains IA, IB, IIA and IIB correspond to subdomains 1, 2, 3 and 4 in actin. Virtually no differences are detectable from the two non-ligand-bound crystal structures (HRES, NATI). Images were created with MOLSCRIPT and RASTER3D[38,39].

Table 1 Refinement statistics

	HRES	NATI	AMPPNP
Residues	4–336	1–336	1–335
Water, cofactor	266	318	0, AMPPNP
Resolution	2.1 Å	2.1 Å	3.1 Å
Twinning fraction*		<0.01	0.055
R-factor, *R*-free†	0.197, 0.234	0.194, 0.240	0.206, 0.276
B average‡	28.6 Å^2	30.3 Å^2	25.2 Å^2
Geometry bonds/angles§	0.006 Å, 1.233°	0.005 Å, 1.264°	0.009 Å, 1.421°
Ramachandran‖	91.5%/0%	94.1%/0%	86.0%/0%
PDB ID¶	1JCE	1JCF	1JCG

*Twinning fraction as used in refinement, operator –h, –k, l.
† Five per cent of reflections were randomly selected for determination of the free *R*-factor (taking twinning into account where appropriate) before any refinement.
‡ Temperature factors averaged for all atoms.
§ r.m.s. deviations from ideal geometry for bond lengths and restraint angles[36].
‖ Percentage of residues in the 'most-favoured region' of the Ramachandran plot and percentage of outliers (PROCHECK[37]).
¶ Protein Data Bank identifiers for coordinates.

entry 1ATN) with an r.m.s. deviation of 3.7 Å over 310 Cα atoms and a *z*-score of 29.2 (ref. 21). MreB and HSC70 (constitutive Hsp70 protein; PDB entry 1HPM) superimpose with an r.m.s. deviation of 3.4 Å over 299 Cα atoms and a *z*-score of 28.8. This gives the impression that MreB is closely related to Hsp70; however, a detailed comparison between the two structures reveals that Hsp70 has a substantial insertion of about 40 residues in subdomain IB, which is absent in MreB and actin. Moreover, Hsp70 contains a principal substrate-binding domain of more than 250 residues at the carboxy-terminus. The other members of the actin superfamily are more distinct: hexokinase (PDB entry 1BDG) has an r.m.s. deviation of 3.5 Å over 253 equivalent residues and a *z*-score of 14.3 when compared to MreB. Bacterial cell-division protein FtsA (PDB entry 1E4G) can be superimposed on MreB with an r.m.s. deviation of 2.8 Å over 270 residues and a *z*-score of 25.2. The fact that FtsA, as a member of the actin family, acts together with the tubulin homologue FtsZ in bacterial cytokinesis suggests that it may also form filaments. However, FtsA does not polymerize into actin-like filaments *in vitro*, as tested under numerous conditions (data not shown). FtsA is distinguished from the other members of the actin family by the position of subdomain IB, which is located on the opposite side of subdomain IA (ref. 14). Another bacterial protein, StbA, which is involved in plasmid segregation is a putative member of the actin superfamily, but is shorter and probably lacks subdomain IIB (ref. 11).

Elucidation of the structure reveals that MreB is most closely related to actin among all members of the actin family. The topology of the secondary structural elements is shared between the two proteins, even in the variable domains IB and IIB (Fig. 4).

Nucleotide-binding site

The nucleotide and the high-affinity, divalent cation-binding sites of MreB are located near the base of the cleft between domains I and II. The superposition of the nucleotide in the MreB structure (AMPPNP) on that of the actin structure (ATP; PDB entry 1YAG) shows that most of the active-site residues are at similar positions,

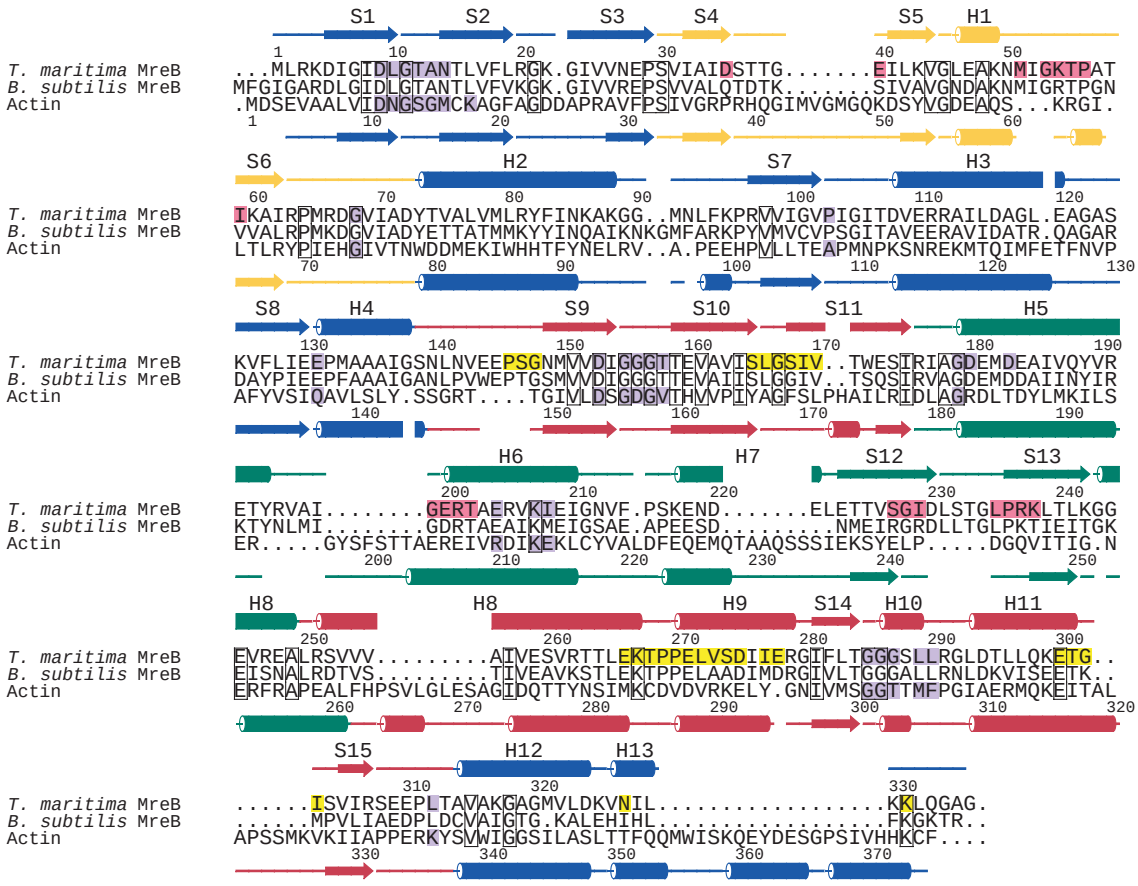

Figure 4 Sequence alignment of MreB1 from *T. maritima* to *B. subtilis* MreB (SWISSPROT: MREB_BACSU) and structure-based sequence alignment to yeast actin (SWISSPROT: ACT_YEAST; PDB, 1YAG) using DALI[21]. Secondary structural elements are shown according to DSSP output of MreB and actin. Helix and strand colours refer to the domain colours in Figs 3 and 5. Active site residues in MreB and actin are highlighted in light purple. Protofilament contacts from one subunit to the next are marked in yellow; residues involved in protofilament contacts to the previous subunit are coloured pink (see residues in Fig. 6). Boxed residues are conserved in all three sequences. Sequence identity is 56% between the two MreB proteins and 15% between MreB and actin. The alignment was prepared with ALSCRIPT[40].

with the exception of the residues located in subdomain IB. These residues, which coordinate the γ-phosphate, are tilted compared with those in actin (see stereo figure in Supplementary Information). This may indicate a different nucleotide state of the two proteins. Most of the residues involved in the coordination of the nucleotide are similar and can be superimposed (purple shaded residues in Fig. 4). Sometimes, where amino acids have changed as in the first phosphate–binding loop (residues 9–14), the interactions are through the amide group of the main chain. Elsewhere, when the residues are different, their role is conserved, as in the hydrophobic pocket that surrounds the adenosine. In actin, the pocket is closed at the top by the hydrophobic part of Glu 214. MreB has Ile 208 at the equivalent position, which has the same role. In addition, actin has a salt bridge between Glu 214 and Arg 210. At the equivalent position of Arg 210, MreB has Glu 204, which forms a salt bridge to Lys 49. This is another example of coevolution, previously reported in a comparison between actin and Hsp70 (ref. 22). The phosphate moiety is bound as in actin, with glycines preceding helix H10 binding to the phosphates. The β-phosphate forms hydrogen bonds with the amides of Ala 13 and Asn 14. The hydrogen bond in actin between Lys 18 and the β-phosphate is not present in MreB, which has a Leu at the equivalent position.

Crystal structure of the MreB protofilament

A notable feature of the crystal packing of both the monoclinic and the trigonal crystal forms is that they contain an MreB protofilament in which the subunits are translated in one dimension (see Supplementary Information for the coordinates of the protofilament). The straight nature of the protofilament is an ideal building block for crystals, which is reflected by the fact that crystals were obtained under many conditions. Most importantly, the spacing between the monomers in the longitudinal direction is identical to the spacing deduced from the electron micrographs (51 Å, Fig. 5). The presence of these protofilaments in both crystal forms and in all of the polymers that were investigated under the electron microscope indicates a high propensity of MreB to form protofilaments. It also proves that intra-protofilament contacts are biologically relevant and not just due to crystal packing.

A closer look at the interface that is formed by two monomers along a protofilament reveals that it is primarily composed of hydrophobic residues (Fig. 6). The two strands S12 (residues 227–229) and S13 (residues 235–238) interact with helix H9 (residues 266–275, 277, 278) and with the loop between helix H11 and strand S15 (residues 300–303). Helix H9 also makes contacts with helix H6 (residues 199–202). The protofilament interface is extended by hydrophobic interactions between residues

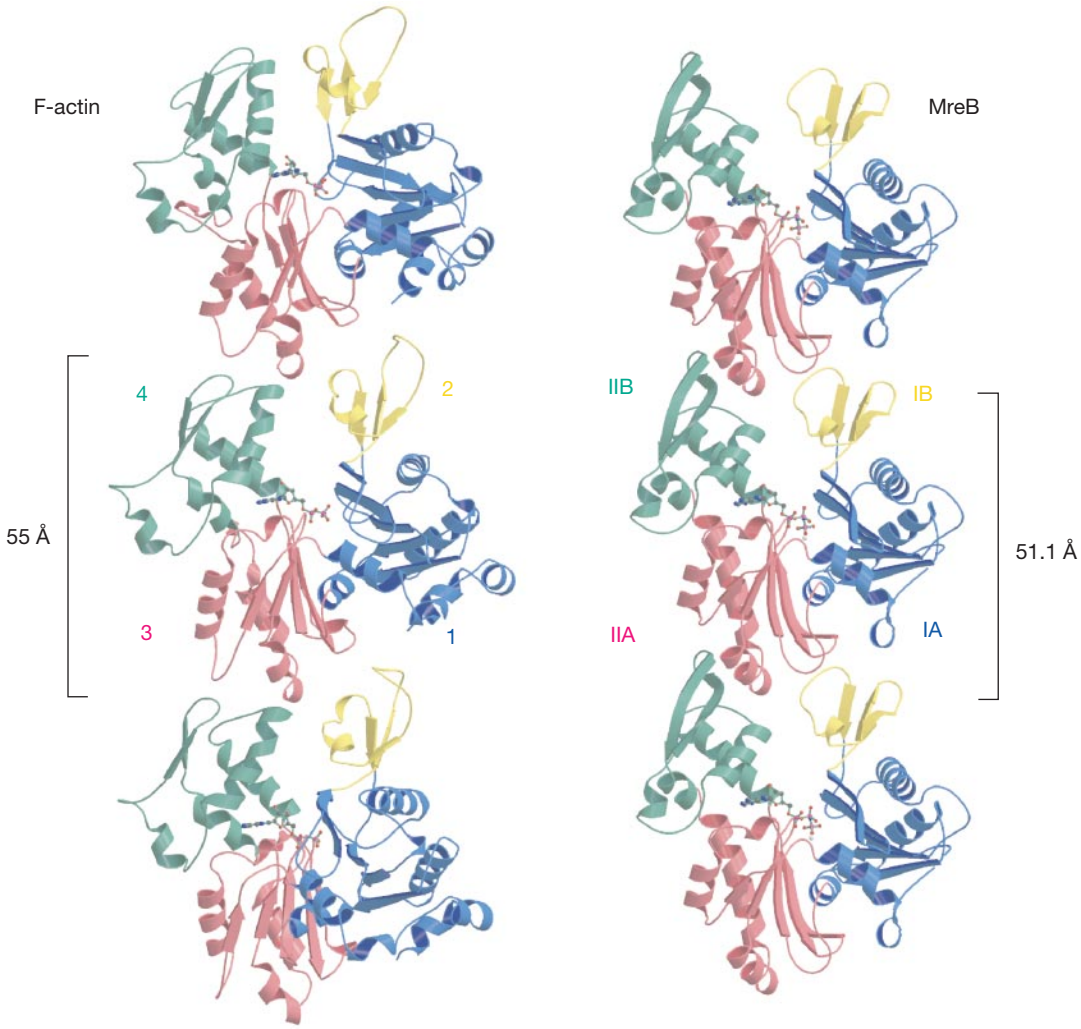

Figure 5 Both crystal forms (HRES, NATI) contain one-dimensional protofilaments. Residues at the bottom of subdomains IA and IIA (1 and 3 in actin) insert into the cleft formed by subdomains IB and IIB (2 and 4 in actin). This is basically the same interaction that has been proposed for the longitudinal interaction in the two strands of F-actin, shown in the left panel[3]. The protofilament repeat is 51.1 Å as measured in crystal form NATI. In the trigonal crystal form the protofilament axis is aligned with the crystallographic cell axis *a*.

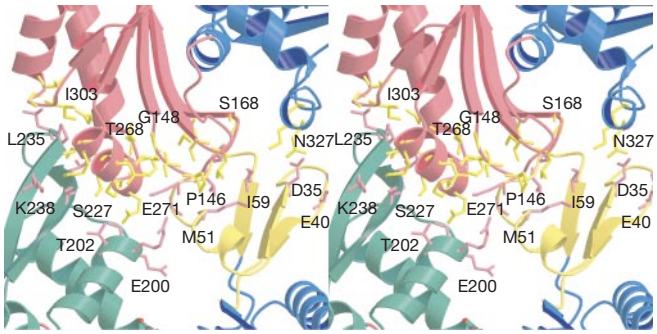

Figure 6 Close-up of the protofilament protein interface. The interaction surface measures 1,709 Å^2, equalling 11.8% of the solvent-accessible surface of monomeric MreB. Residues are coloured as in Fig. 4 with yellow for those involved in contacts from one subunit to the one above, and pink for contacts to the subunit below. The image was created with MOLSCRIPT and RASTER3D[38,39].

from the loop connecting helix H1 with strand S6 (residues 51–59) and the two loops preceding strands S9 (residues 146–148) and S11 (residues 165–170). Hydrophilic interactions between Lys 330 and Asp 40, as well as Lys 331 and Asp 35, complete the interface.

The resemblance between actin and MreB is reflected in the structure of the filament as well as in the longitudinal repeat (Fig. 5). In addition, actin and MreB are in almost identical orientation in the protofilament, resulting in the same longitudinal contact region. A discrepancy between F-actin and the filaments of MreB is that F-actin is a twisted pair of protofilaments. It is possible that the twist is imposed by different lateral interactions in actin, such as those from the actin-specific loop inserted in H8. In any case, the lateral interactions in actin are variable as the twisted parallel arrangement of the protofilaments in F-actin can be converted into the straight antiparallel organization in the actin sheets[6]. The filtered image of an MreB sheet (Fig. 2g) can also be explained by a side view of adjacent protofilaments (Fig. 2h). At the present resolution, the protofilaments do not show a definite polarity; adjacent protofilaments in the sheets are not obviously different. Cryo-electron microscopy is needed for a detailed analysis of the arrangement of the protofilaments in both sheets and filaments.

We present here an actin-like protofilament in atomic detail. Because the current model of F-actin is of low resolution, a detailed comparison between the protofilament interface of MreB and actin is not possible at the moment. Interestingly, the refined model of F-actin[23,24] is less similar to our crystal structure than the initial unrefined model, in which the crystal structure of G-actin in complex with DNase I was used[3]. This finding is supported by the fact that the significant conformational changes in the refined F-actin model are inconsistent with the structural changes identified in the analysis of domain movements made on the basis of four different crystal structures of actin[25].

Although it is impossible to compare the protofilament interface in detail, the structure-based sequence alignment between MreB and actin shows that the residues involved in the monomer contacts along the protofilament are not well conserved (Fig. 4). Apparently, evolution has allowed for (concomitant) mutations of residues on both sides of the interface. A low degree of conservation in the protofilament interface has also been found for filaments of FtsZ and tubulin[26].

Previous studies implicated MreB in the determination of cell shape in bacteria and showed MreB-dependent cytosketetal structures[20], suggesting a functional similarity between MreB and actin. To further support this relationship, future experiments are needed, which may shed light on the dynamic behaviour of MreB. It remains to be seen whether MreB shares other properties with actin such as treadmilling, or forming a track for motor proteins. Nevertheless, the biochemical and structural data presented here strongly suggest that MreB is an excellent candidate for the actin homologue in bacteria. □

Methods

Protein expression and purification

The two MreB homologues from *T. maritima* (DSMZ number 3109: MreB1, TM0588 (SWALL: Q9WZ57); MreB2, TM1544 (SWALL: Q9X1N0)) were amplified by genomic PCR using primers that introduce unique cleavage sites for *Nde*I and *Bam*HI into the product. The fragments were cloned into pHis17. This enables the proteins to be expressed under the control of the T7 promoter and adds eight residues to the C-terminus (GSHHHHHH). C41(DE3) cells[27] were transformed, grown at 37 °C and induced in log phase (A_{600} = 0.6) with 1 mM IPTG. The cells were collected after 4 h induction, and the pellets were frozen in liquid nitrogen. Cells were thawed and lysed by the addition of lysozyme and subsequent sonication, in a buffer of 50 mM Tris-HCl pH 8.0. DNase I was added and after centrifugation (140,000*g*) the lysate was applied to a Ni^{2+}-NTA column (QIAGEN). Buffer A was 300 mM NaCl and 50 mM Tris-HCl pH 6.0; buffer B was 1 M imidazole and 50 mM Tris-HCl, pH 6.0. After washing with 5% buffer B the protein was eluted with 30% buffer B. Peak fractions were pooled and concentrated before loading onto a sephacryl S200 column (Amersham-Pharmacia) equilibrated in 20 mM Tris-HCl, 200 mM NaCl, 1 mM EDTA and 1 mM NaN_3, pH 7.5.

Polymerization assays

Purified *T. maritima* MreB (35.8K) was mixed in a volume of 40 μl with 100 mM Tris-HCl, pH 7.0, 2 mM nucleotides, 4 mM $MgCl_2$ and 100 mM NaCl, and incubated at 37 °C for 30 min, if not stated otherwise. Final protein concentration was 1 mg ml^{-1} (28 μM). (For exact conditions please refer to legend of Fig. 1a, b.) The reactions were centrifuged at 140,000*g* in a Beckman TLA100 rotor for 20 min at 20 °C. The supernatant was removed for analysis and the pellet washed with buffer containing the same components as the reaction buffer minus protein. Pellets were solubilized with SDS-containing gel loading buffer, using the same volume as for the supernatant. Samples were analysed on 12% SDS–polyacrylamide gel electrophoresis (PAGE) gels.

Electron microscopy

MreB at 1 mg ml^{-1} in polymerization buffer (see Fig. 2 legend) was incubated at 37 °C for 30 min. Next, 5 μl of the reaction was put on carbon-coated copper electron microscopic grids. Excess liquid was blotted off. Grids were washed with a drop of water, stained with 2% uranyl acetate solution and dried. Pictures were taken with a Philips 208 electron microscope on film plates at ×40,000–80,000 magnification. Images were digitized on a Zeiss SCAI CCD scanner at 21–28-μm resolution, and analysed using MRC image processing software[28].

Crystallization and structural determination

Seleno-methionine (SeMet)-substituted MreB protein was expressed as described[29]. For purification of SeMet-substituted protein, buffers A and B contained 5 mM β-mercapto-ethanol, and the final buffer contained 5 mM dithiothreitol. Native crystals were grown using the sitting-drop vapour diffusion technique using 10% PEG 8000, 200 mM NaCl and 0.1 M CAPS, pH 10.5 as the crystallization solution. Drops composed of 1 μl protein at 8 mg ml^{-1} and 1 μl crystallization solution were equilibrated for a minimum of 3 days at 19 °C. Seleno-methionine-substituted crystals were grown in the same manner as for the native protein but with 10% isopropanol, 200 mM NaCl and 0.1 M HEPES, pH 7.5. Crystals were frozen in mother liquor complemented with 25% PEG400 or 30% glycerol for the native and SeMet crystals, respectively. Crystals belong to space group $P3_121$ (native) or *C*2 (SeMet). Two SeMet MAD datasets and the native dataset were collected at ID14-4, ESRF, Grenoble (see Supplementary Information Table 1). Crystals were indexed and integrated using the MOSFLM package[30], and data were further processed using the CCP4 package[31].

An initial 2.4 Å MAD density map was generated by locating eight selenium sites using the program SOLVE[32], which was also used to calculate phases. Final figure of merit of the phases was 0.7 for all data to 2.4 Å resolution. We used RESOLVE[33] for solvent flattening, assuming 60% solvent content. All ordered residues were built into the MAD electron density map using MAIN[34]. The structure was refined against all data in dataset HRES (SeMet inflection point) to 2.1 Å resolution using CNS[35], taking anomalous and dispersive terms for the selenium atoms into account. Dataset NATI showed weak twinning when comparing cumulative intensity distributions with those from randomly scattered atoms (TRUNCATE). However, the twinning fraction was found to be less than 1% after refinement, and was ignored. NATI was solved by molecular replacement using the refined HRES model and AMORE. Dataset AMPPNP was collected in-house from a trigonal crystal soaked for 2–3 h in mother liquor supplemented with 2 mM AMPPNP and 4 mM $MgCl_2$. The crystal was isomorphous to NATI and the structure was solved by difference Fourier methods, clearly showing the difference density for AMPPNP and magnesium. Details of the refined models are summarized in Table 1.

Received 13 June; accepted 2 August 2001.

1. Schmidt, A. & Hall, M. N. Signaling to the actin cytoskeleton. *Annu. Rev. Cell Dev. Biol.* **14,** 305–338 (1998).
2. Straub, F. B. Actin. *Stud. Inst. Med. Chem. Univ. Szeged* **2,** 3–15 (1942).

3. Holmes, K. C., Popp, D., Gebhard, W. & Kabsch, W. Atomic model of the actin filament. *Nature* **347,** 44–49 (1990).
4. Egelman, E. H., Francis, N. & DeRosier, D. J. F-actin is a helix with a random variable twist. *Nature* **298,** 131–135 (1982).
5. Steinmetz, M. O. *et al.* An atomic model of crystalline actin tubes: combining electron microscopy with X-ray crystallography. *J. Mol. Biol.* **278,** 703–711 (1998).
6. Aebi, U., Fowler, W. E., Isenberg, G., Pollard, T. D. & Smith, P. R. Crystalline actin sheets—their structure and polymorphism. *J. Cell Biol.* **91,** 340–351 (1981).
7. Kabsch, W., Mannherz, H. G., Suck, D., Pai, E. F. & Holmes, K. C. Atomic-structure of the actin–DNase-I complex. *Nature* **347,** 37–44 (1990).
8. McLaughlin, P. J., Gooch, J. T., Mannherz, H. G. & Weeds, A. G. Structure of gelsolin segment-1-actin complex and the mechanism of filament severing. *Nature* **364,** 685–692 (1993).
9. Schutt, C. E., Myslik, J. C., Rozycki, M. D., Goonesekere, N. C. W. & Lindberg, U. The structure of crystalline profilin β-actin. *Nature* **365,** 810–816 (1993).
10. Chik, J. K., Lindberg, U. & Schutt, C. E. The structure of an open state of β-actin at 2.65 angstrom resolution. *J. Mol. Biol.* **263,** 607–623 (1996).
11. Bork, P., Sander, C. & Valencia, A. An ATPase domain common to prokaryotic cell-cycle proteins, sugar kinases, actin, and Hsp70 heat-shock proteins. *Proc. Natl Acad. Sci. USA* **89,** 7290–7294 (1992).
12. Kabsch, W. & Holmes, K. C. Protein motifs 2. The actin fold. *FASEB J.* **9,** 167–174 (1995).
13. Flaherty, K. M., Delucaflaherty, C. & McKay, D. B. Three-dimensional structure of the ATPase fragment of a 70kDa heat-shock cognate protein. *Nature* **346,** 623–628 (1990).
14. van den Ent, F. & Löwe, J. Crystal structure of the cell division protein FtsA from *Thermotoga maritima*. *EMBO J.* **19,** 5300–5307 (2000).
15. Hurley, J. H. *et al.* Structure of the regulatory complex of *Escherichi coli* Iii(Glc) with glycerol kinase. *Science* **259,** 673–677 (1993).
16. Anderson, C. M., McDonald, R. C. & Steitz, T. A. Sequencing a protein by X-ray crystallography. Interpretation of yeast hexokinase B at 2.5 Å resolution by model building. *J. Mol. Biol.* **123,** 1–13 (1978).
17. Wachi, M. *et al.* Mutant isolation and molecular cloning of *mre* genes, which determine cell shape, sensitivity to mecillinam, and amount of penicillin-binding proteins in *Escherichia coli*. *J. Bacteriol.* **169,** 4935–4940 (1987).
18. Doi, M. *et al.* Determinations of the DNA sequence of the *mreB* gene and of the gene products of the *mre* region that function in formation of the rod shape of *Escherichia coli* cells. *J. Bacteriol.* **170,** 4619–4624 (1988).
19. Levin, P. A., Margolis, P. S., Setlow, P., Losick, R. & Sun, D. X. Identification of *Bacillus subtilis* genes for septum placement and shape determination. *J. Bacteriol.* **174,** 6717–6728 (1992).
20. Jones, L. J. F., Carballido-Lopez, R. & Errington, J. Control of cell shape in bacteria: helical, actin-like filaments in *Bacillus subtilis*. *Cell* **104,** 913–922 (2001).
21. Holm, L. & Sander, C. Protein structure comparison by alignment of distance matrices. *J. Mol. Biol.* **233,** 123–138 (1993).
22. Flaherty, K. M., McKay, D. B., Kabsch, W. & Holmes, K. C. Similarity of the 3-dimensional structures of actin and the ATPase fragment of a 70-kDa heat-shock cognate protein. *Proc. Natl Acad. Sci. USA* **88,** 5041–5045 (1991).
23. Lorenz, M., Popp, D. & Holmes, K. C. Refinement of the F-actin model against X-ray fiber diffraction data by the use of a directed mutation algorithm. *J. Mol. Biol.* **234,** 826–836 (1993).
24. Tirion, M. M., Benavraham, D., Lorenz, M. & Holmes, K. C. Normal-modes as refinement parameters for the F-actin model. *Biophys. J.* **68,** 5–12 (1995).
25. Page, R., Lindberg, U. & Schutt, C. E. Domain motions in actin. *J. Mol. Biol.* **280,** 463–474 (1998).
26. Nogales, E., Downing, K. H., Amos, L. A. & Löwe, J. Tubulin and FtsZ form a distinct family of GTPases. *Nature Struct. Biol.* **5,** 451–458 (1998).
27. Miroux, B. & Walker, J. E. Over-production of proteins in *Escherichia coli*: mutant hosts that allow synthesis of some membrane proteins and globular proteins at high levels. *J. Mol. Biol.* **260,** 289–298 (1996).
28. Crowther, R. A., Henderson, R. & Smith, J. M. MRC image processing programs. *J. Struct. Biol.* **116,** 9–16 (1996).
29. van den Ent, F., Lockhart, A., Kendrick-Jones, J. & Löwe, J. Crystal structure of the N-terminal domain of MukB: a protein involved in chromosome partitioning. *Struct. Fold. Des.* **7,** 1181–1187 (1999).
30. Leslie, A. G. W. *Recent Changes to the MOSFLM Package for Processing Film and Image Plate Data* (SERC Laboratory, Daresbury, UK, 1991).
31. Collaborative Computing Project No. 4. The CCP4 suite: Programs for protein crystallography. *Acta Crystallogr. D* **50,** 760–763 (1994).
32. Terwilliger, T. C. & Berendzen, J. Automated MAD and MIR structure solution. *Acta Crystallogr. D* **55,** 849–861 (1999).
33. Terwilliger, T. C. Maximum-likelihood density modification. *Acta Crystallogr. D* **56,** 965–972 (2000).
34. Turk, D. *Weiterentwicklung eines Programms für Molekülgrafik und Elektrondichte-Manipulation und seine Anwendung auf verschiedene Protein-Strukturaufklärungen.* Thesis, Technische Univ. München (1992).
35. Brünger, A. T. *et al.* Crystallography & NMR system: a new software suite for macromolecular structure determination. *Acta Crystallogr. D* **54,** 905–921 (1998).
36. Engh, R. A. & Huber, R. Accurate bond and angle parameters for X-ray protein structure refinement. *Acta Crystallogr. A* **47,** 392–400 (1991).
37. Laskowski, R. A., MacArthur, M. W., Moss, D. S. & Thornton, J. M. Procheck—a program to check the stereochemical quality of protein structures. *J. Appl. Crystallogr.* **26,** 283–291 (1993).
38. Kraulis, P. J. MOLSCRIPT: a program to produce both detailed and schematic plots of protein structures. *J. Appl. Crystallogr.* **24,** 946–950 (1991).
39. Merritt, E. A. & Bacon, D. J. Raster 3D: photorealistic molecular graphics. *Methods Enzymol.* **277,** 505–524 (1997).
40. Barton, G. J. ALSCRIPT: a tool to format multiple sequence alignments. *Protein Eng.* **6,** 37–40 (1993).

Supplementary information is available on *Nature*'s World-Wide Web site (http://www.nature.com) or as a paper copy from the London editorial office of *Nature*.

Acknowledgements

We would like to thank S. Munro for critically reading the manuscript and the staff at ID14-4 of ESRF (Grenoble, France) for assistance with MAD data collection.

Correspondence and requests for materials should be addressed to F.V.D.E. (e-mail: fent@mrc-lmb.cam.ac.uk). The coordinates for HRES (space group *C*2), NATI (space group $P3_121$) and AMPPNP are deposited in the Protein Data Bank under accession numbers 1JCE, 1JCF and 1JCF, respectively.